Single-cell analysis of the CD8$^+$ T-cell compartment in multiple myeloma reveals disease specific changes are chiefly restricted to a CD69$^-$ subset suggesting potent cytotoxic effectors exist within the tumor bed

James Favaloro,[1,2*] Christian E. Bryant,[1,3*] Edward Abadir,[1,3] Samuel Gardiner,[4] Shihong Yang,[1] Tracy King,[1,3] Najah Nassif,[2] Lisa M. Sedger,[5,6] Richard Boyle,[7] Douglas E. Joshua[1,3] and P. Joy Ho[1,2,3]

[1]Institute of Hematology, Multiple Myeloma Research Laboratory, New South Wales Health Pathology, Royal Prince Alfred Hospital, Camperdown; [2]School of Life Sciences, University of Technology Sydney, Ultimo, Sydney; [3]Sydney Medical School, the University of Sydney, Sydney; [4]Sydney Local Health District Clinical Research Institute, Royal Prince Alfred Hospital, Camperdown; [5]Institute for Clinical Pathology and Medical Research (ICPMR), New South Wales Health Pathology, Westmead Hospital, Westemead; [6]Center for Virus Research, Westmead Institute for Medical Research, Westmead and New South Wales, Sydney and [7]Orthopedics Department, Sydney Local Health District, Royal Prince Alfred Hospital, Camperdown, New South Wales, Australia

JF and CEB contributed equally as first authors.

Correspondence: J. Favaloro
james.favaloro@health.nsw.gov.au

C.E. Bryant
christian.bryant@health.nsw.gov.au.

Received: May 14, 2023.
Accepted: September 28, 2023.
Early view: October 5, 2023.

https://doi.org/10.3324/haematol.2023.283062

©2024 Ferrata Storti Foundation
Published under a CC BY-NC license

Supplementary

Table of Contents

Supplementary methods

Single-cell RNA sequencing

Purified $CD8^+$ cells were isolated from cryopreserved, paired BM and PB samples through a two-stage enrichment using a human $CD8^+$ T-cell Isolation Kit (Miltenyi Biotech) followed by FACS sorting as $CD45^+CD8^+CD4^-CD56^-$ cells on a BD FACS Aria II. Single cells were encapsulated for cDNA synthesis and barcoded using the Chromium Single-cell 5' V(D)J Reagent kit v1.1 (10x Genomics) followed by library construction according to the manufacturer's recommendations. The quality and quantity of libraries were determined using an Agilent 2100 Bioanalyzer with 2100 Expert version B.02.11.SI811 software and a High Sensitivity DNA kit. Libraries were sequenced on an Illumina NovaSeq 6000 (NovaSeq Control Software v.1.6.0 / Real-Time Analysis v.3.4.4) using a NovaSeq S4 reagent kit (Illumina) as follows: 28bp (Read 1), 91bp (Read 2) and 8bp (Index)) at a sequencing depth of ~50,000 reads per cell, followed by computational alignment using CellRanger[1] (version 3.10, 10x Genomics). Subsequently, datasets were subjected to quality control steps using Seurat[2] (version 4.0.4) that included selecting cells with a library complexity of more than 200 features, expressing at least 3 common genes, removing doublets and poor-quality cells (cells with ± 1.5 SD the amounts of unique molecular identifiers (UMIs) percentages of mitochondrial genes). TCR, mitochondrial and ribosomal genes were removed before downstream analyses. QC revealed poor-quality transcriptomic data for two patient samples, which were excluded from further analysis reliant on paired BM/PB samples, although the V(D)J data for these patients was acceptable and used for downstream analysis (Supp. Table 3) which will be published separately.

For initial interrogation, data from paired BM and PB samples from two individuals with myeloma were merged by integration and label transfer, normalized using SCTransform and analyzed by PCA on the 3000 most variable genes (excluding TCR genes). Unsupervised clustering was performed on the top 10 PC using a shared nearest neighbor (SNN) modularity optimization-based clustering algorithm (resolution 0.2) integrated into Seurat, and cells were projected in two dimensions using UMAP.[3] Differential expression testing was performed using the Wilcox method implemented by the "FindMarkers" function of Seurat and ranked according to log2FC. Generation of MM reference atlases was performed using ProjecTILs[4] (version 2.0.3). Briefly, BM from two, and PB from four individuals with untreated myeloma were subjected to the same pre-processing and then transformed into reference atlases using the same PCA/UMAP parameters. In addition to generated data, publicly available scRNA-Seq data from Szabo, et al., 2019[5], comprising paired BM and PB samples in both resting and TCR-activated states from two age-matched controls, were processed and analyzed.

Cluster names were designated through a combination of inference with SingleR[6] (version 1.10.0) and expression of canonical genes. Sc-GSEA) was performed using escape[7] (version 1.6.0) using the predefined gene sets from the Molecular Signatures Database (MSigDB,[8] version 7.5.1). Analysis scripts are available at https://github.com/JFavaloro.

Mass cytometry and FlowSOM analysis of the CD8$^+$ T_{EM} subset

BM MNCs and PB MNCs from MGUS (n = 4) and NDMM (n = 8) patients were analyzed by mass cytometry as previously described.[9] A negative gating strategy, consistent with previously published work,[9] was used to identify CD8$^+$ T_{EM} (Supp. Figure 1) before being imported into R and analyzed as previously described.[10] t-distributed stochastic neighbor embedding (tSNE) plots were generated using the same 13 antigens selected for FlowSOM analysis (Supp. Table 2). This same method was additionally undertaken using flow cytometry data.

Supplementary Figures

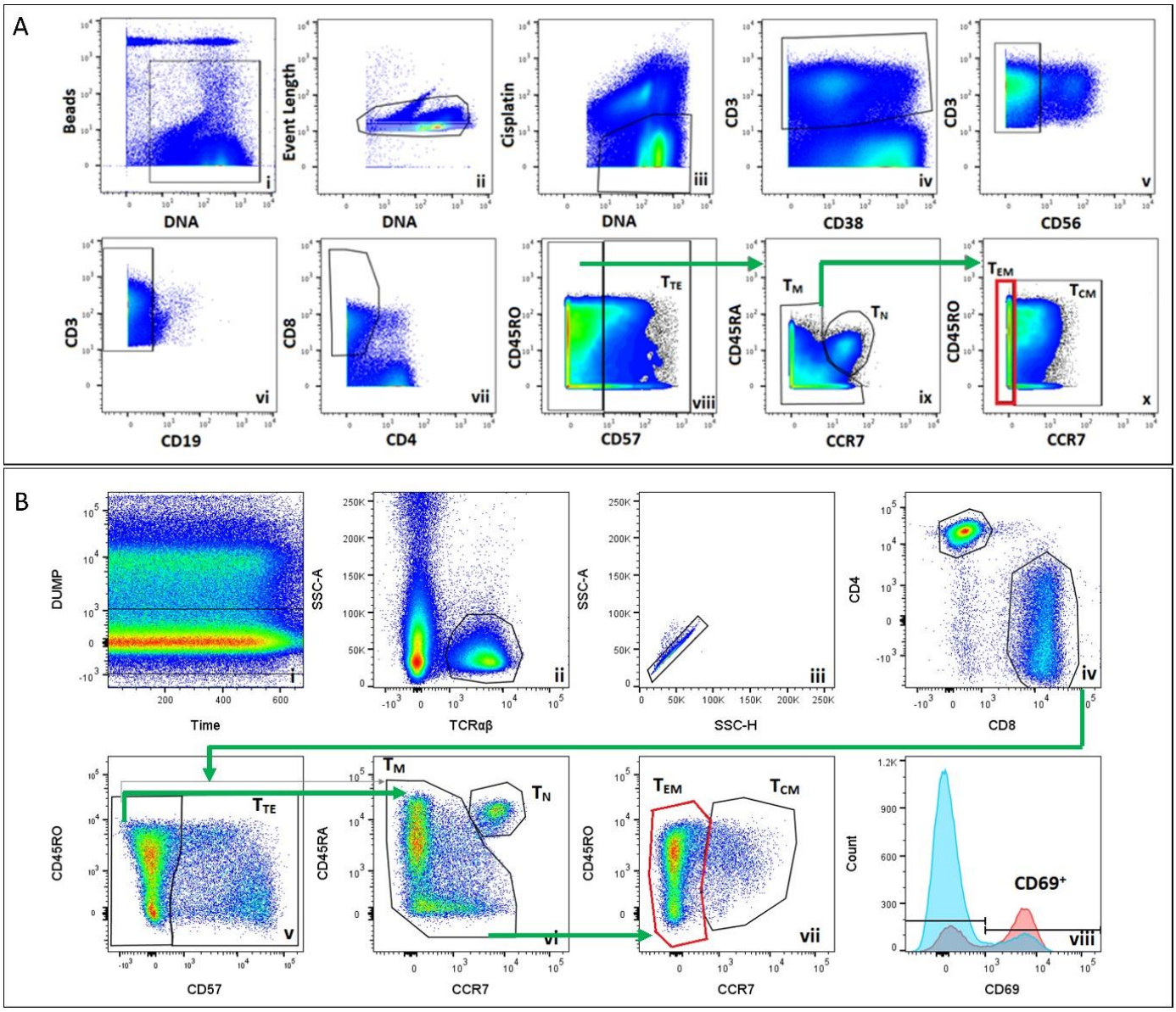

Supp. Figure 1: Identification of the four canonical CD8⁺ T-cell subsets by manual gating of A) mass cytometry and B) flow cytometry data. A). Viable single cells were identified by excluding beads (i), doublets (ii) and dead cells (iii). $CD8^+$ T-cells were identified by excluding $CD38^+CD3^-$ PCs (iv), $CD56^+$ NK-cells (v), $CD19^+$ B-cells (vi) and $CD4^+$ T-cells (vii). $CD8^+$ T_{EM} cells were identified by excluding $CD8^+CD57^+$ T_{TE} cells (viii), $CCR7^+CD45RA^+$ T_N cells (ix) and finally excluding the $CCR7^+CD45RO^{+/-}$ T_{CM} population by gating on the $CCR7^-CD45RO^{+/-}$ T_{EM} population (x) (indicated by the red rectangle). Arrows represent gating hierarchy. **B)** Viable T-cells were identified by excluding $Dump^+$ events ($CD14^+CD19^+CD56^+FVS700^+$) (i), gating $TCR\alpha\beta^+$ (ii) singlets (iii). $CD8^+$ T-cell subsets were identified by separating $CD45RO^{+/-}CD57^+$ T_{TE} (v) from remaining cells into $CD45RA^+CCR7^+$ TN and remaining T_M cells (vi) and then into $CD45RO^{+/-}CCR7^-$ T_{EM} (indicated by the red polygon gate) and $CD45RO^{+/-}CCR7^+$ T_{CM} (vii). In some analyses the proportion of cells expressing CD69 were then determined, in others cells were split first on the basis of CD69 and then the proportion of T-cell subsets determined using the above described hierarchy. Arrows represent gating hierarchy.

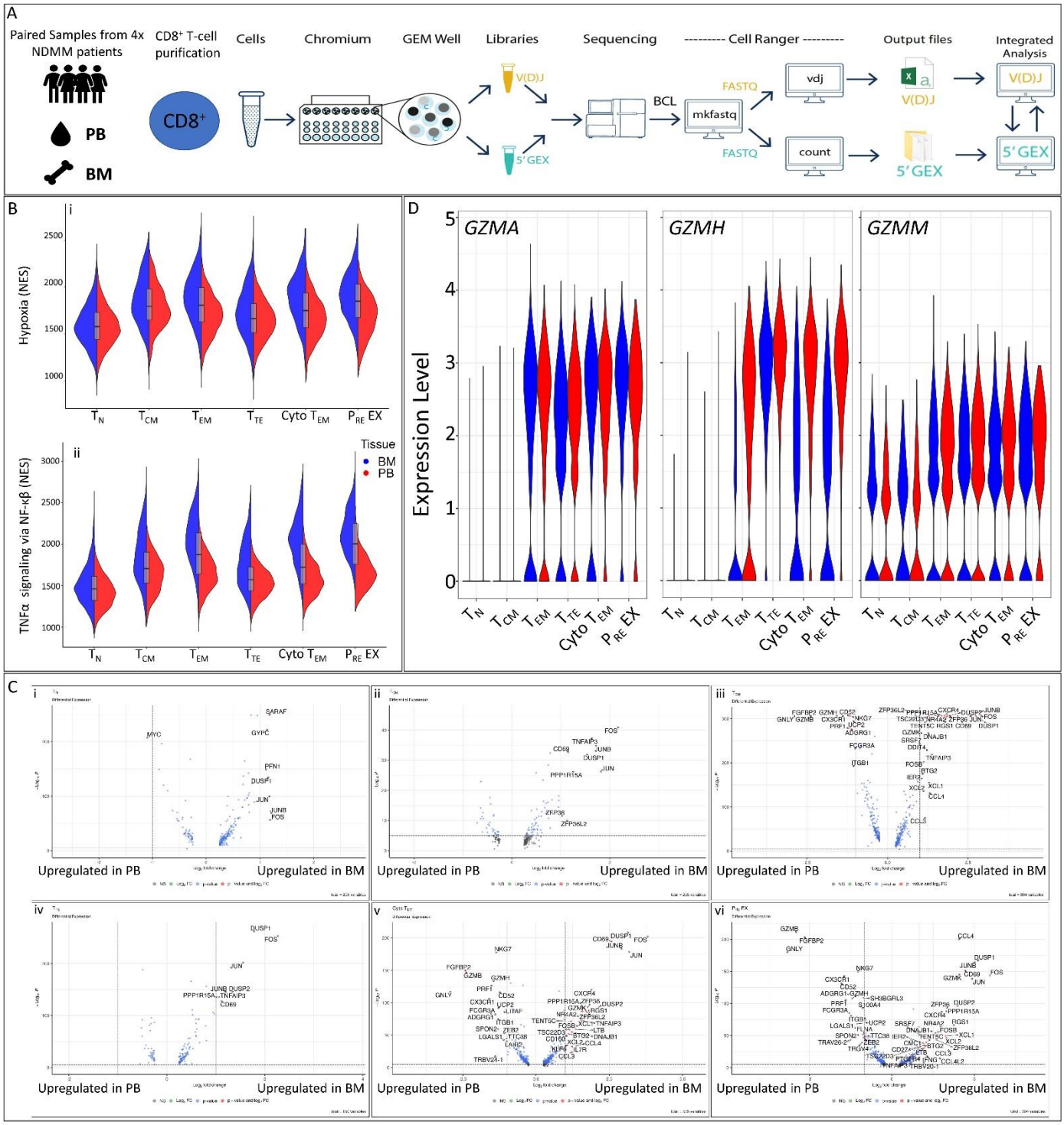

Supp. Figure 2. Additional scRNA-Seq figures. A) Experimental design. CD8⁺ T-cells from paired BM/PB samples from four NDMM patients were isolated in a two-stage process and subjected to scRNA-seq and scTCR-seq using the 10x genomics platform. Stringent QC (detailed in the supplementary methods) revealed poor quality data for two BM samples which were excluded from further analysis. **B) Split violin plots** showing normalized enrichment scores (NES) toward the hallmark gene sets of (i) hypoxia and (ii) TNFα signaling via NF-κβ in the BM (blue) and PB (red). The median, upper and lower quartiles are illustrated relative to cluster expression without segregation of tissue. **C) Volcano plots** illustrating differential expression results comparing the BM to the PB across the (i) T_N, (ii) T_{CM}, (iii) T_{EM}, (iv) T_{TE}, (v) Cytotoxic T_{EM} and (vi) P_{RE}-Exhausted clusters. Red dots (annotated) represent genes that are both significantly upregulated and expressed at a Log_2 FC value of >1 in the BM (right) relative to the PB or <1 in the PB (left) relative to the BM. Blue dots represent genes that are significantly different but not expressed at a great enough level (i.e., >1 or <1 Log_2 FC). Green dots represent genes that are highly expressed (i.e., >1 or <1 Log_2 FC) but found to be not significantly differentially expressed between the two tissues. Black dots represent tested genes that are neither highly expressed nor significantly different between the two tissues. **D) Violin plots** showing expression levels (y-axis) of *GZMA* (left), *GZMH* (middle), and *GZMM* (right) across the six identified clusters, separated by tissue (BM = blue, PB = red).

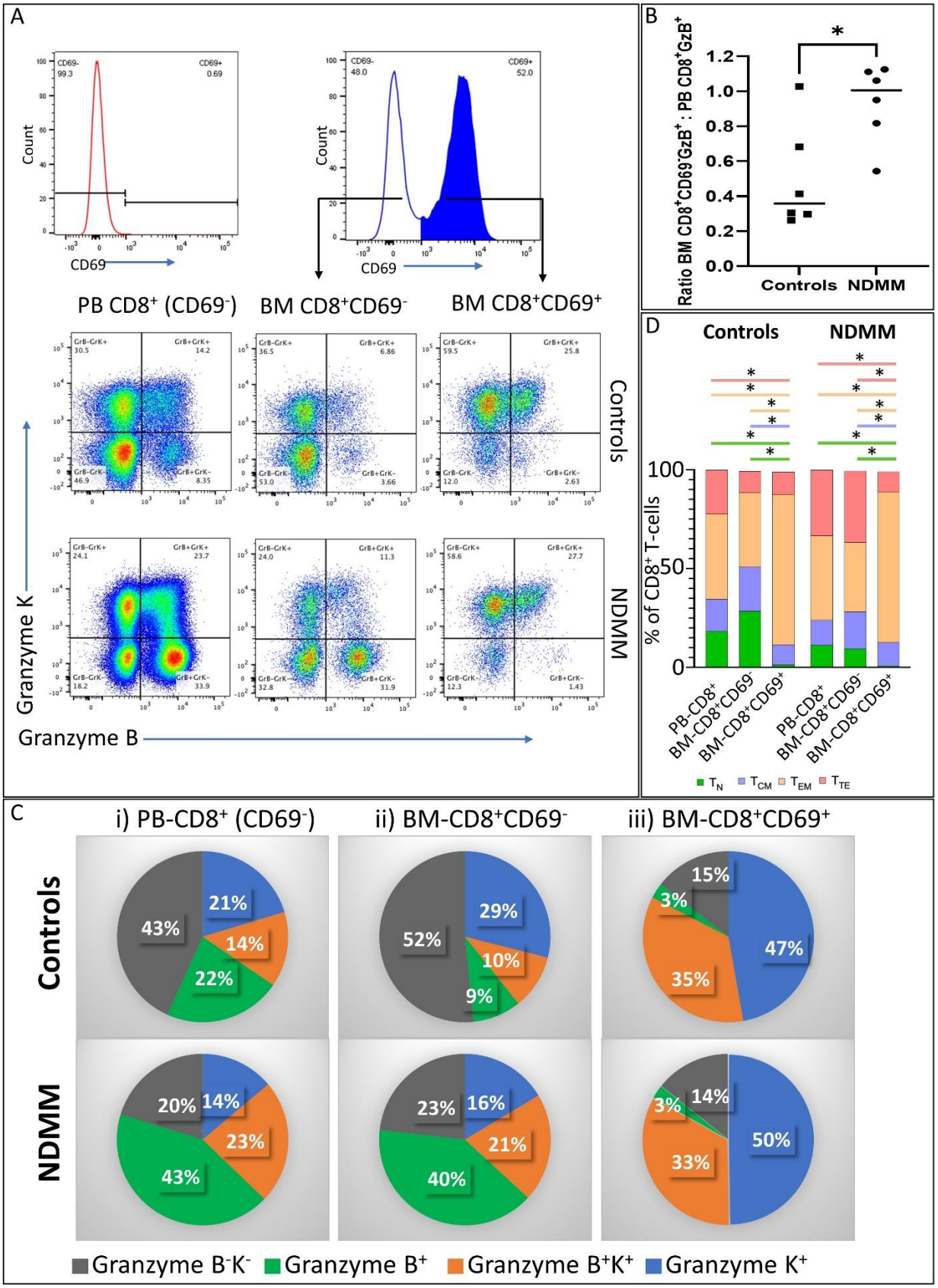

Supp. Figure 3: Additional flow cytometry figures: Granzyme expression. A) Representative flow plots from an age-matched control (top row) and NDMM patient (bottom row) demonstrating the distribution of Granzyme B and Granzyme K across PB-CD8$^+$ (left), BM-CD8$^+$CD69$^-$ (middle) and BM-CD8$^+$CD69$^+$ T-cells (right). **B)** Ratio (BM-CD8$^+$CD69$^-$: PB-CD8$^+$) of Granzyme B single positive cells in age-matched controls (left, squares) and NDMM patients (right, circles)**. C)** Pie charts illustrating average proportions of Granzyme K$^-$/B$^-$ (grey), Granzyme B$^+$ (green), Granzyme B$^+$/K$^+$ (orange), or Granzyme K$^+$ (blue) in (i) PB-CD8$^+$, (ii) BM-CD8$^+$CD69$^-$ and (iii) BM-CD8$^+$CD69$^+$ T-cell subsets in age-matched controls (n = 6; top) and NDMM patients (n = 6; bottom). **D)** Stacked bar graph demonstrating the distribution of canonical CD8$^+$ T-cell subsets in age-matched controls (left) and NDMM patients (right) across the PB-CD8$^+$, BM-CD8$^+$CD69$^-$ and BM-CD8$^+$CD69$^+$ T-cell subsets. Significance levels: *p <0.05, Mann-Whitney U-test (Figure B), *p <0.05, Wilcoxon matched-pairs signed-rank test (Figure C).

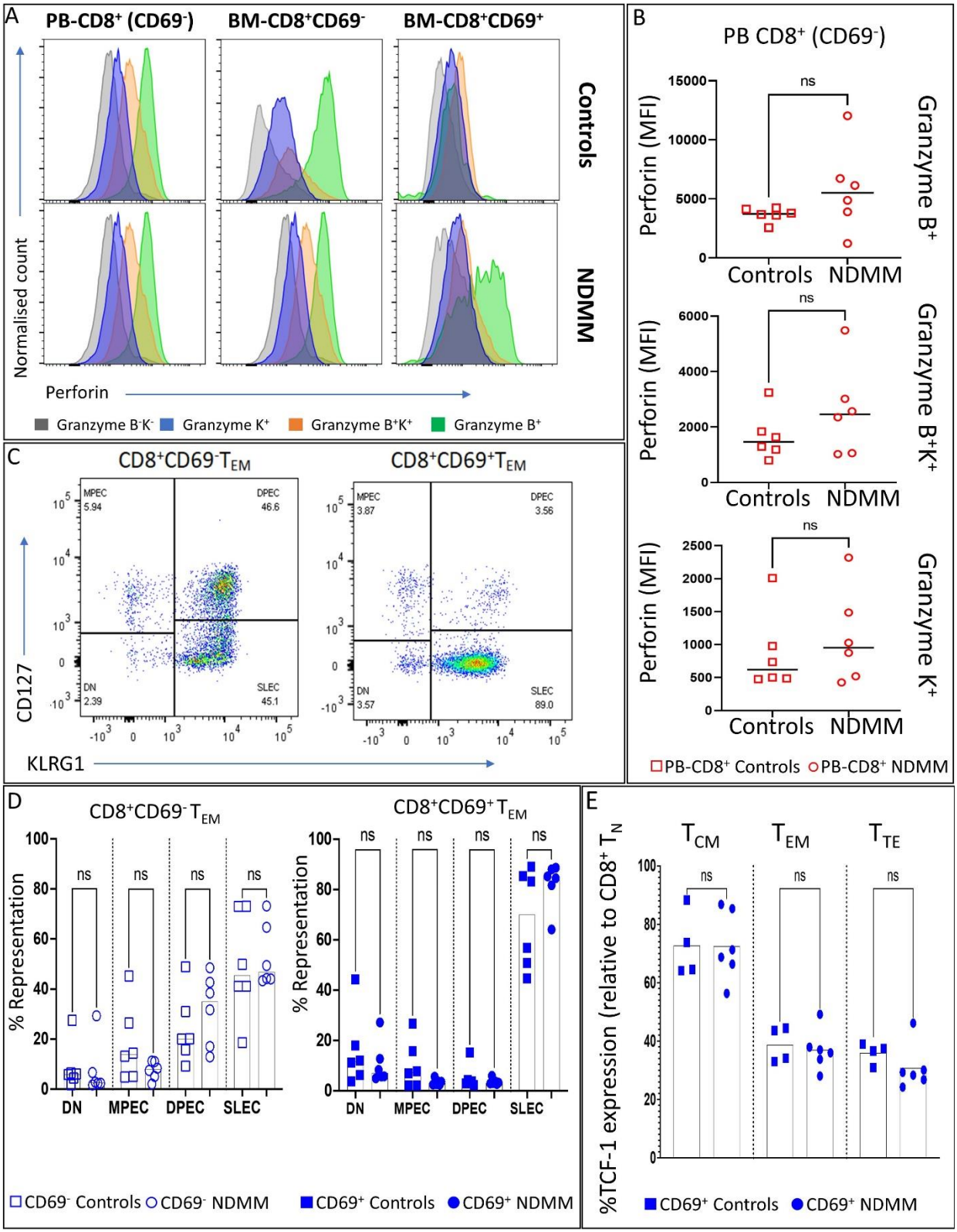

Supp. Figure 4: Additional flow cytometry figures: Perforin, TCF-1 expression, and effector/memory subsets. A) Representative histograms of Perforin expression in the Granzyme K$^+$ (blue), Granzyme B$^+$/K$^+$ (orange), Granzyme B$^+$ (green) or Granzyme K$^-$/B$^-$ (grey) subsets across the PB-CD8$^+$ (left), BM-CD8$^+$CD69$^-$ (middle), BM-CD8$^+$CD69$^+$ (right) T-cell subsets in an age-matched control (top) and NDMM patient (bottom). **B)** MFI of Perforin expression across the Granzyme B$^+$ (top) Granzyme B$^+$/K$^+$ (middle) or Granzyme K$^+$ (bottom) subsets in the PB of age-matched controls (left; hollow red squares; n = 6) and NDMM patients (right; hollow red circles; n = 6). **C)** Representative flow plot of one NDMM patient showing distribution of CD127 (IL7R) and KLRG1 across the BM-CD8$^+$CD69$^-$ (left) and BM-CD8$^+$CD69$^+$ (right) T_{EM} subsets. **D)** Bar plots (median with individual values) showing distribution of effector/memory subsets in the BM-CD8$^+$CD69$^-$ (left, open shapes) and BM-CD8$^+$CD69$^+$ (right, solid shapes) T_{EM} subsets in age-matched controls (squares) and NDMM patients (circles). **E)** TCF-1 expression on canonical CD8$^+$ T-cell memory subsets as a proportion of the expression level (MFI) in the T_N subset between age-matched controls (n = 4, squares) and NDMM (n = 6, circles). DN; Double Negative; MPEC; Memory Precursor Effector Cells, DPEC; Double Positive Effector Cells, SLEC; Short Lived Effector Cells, MFI; Median Fluorescence Intensity.

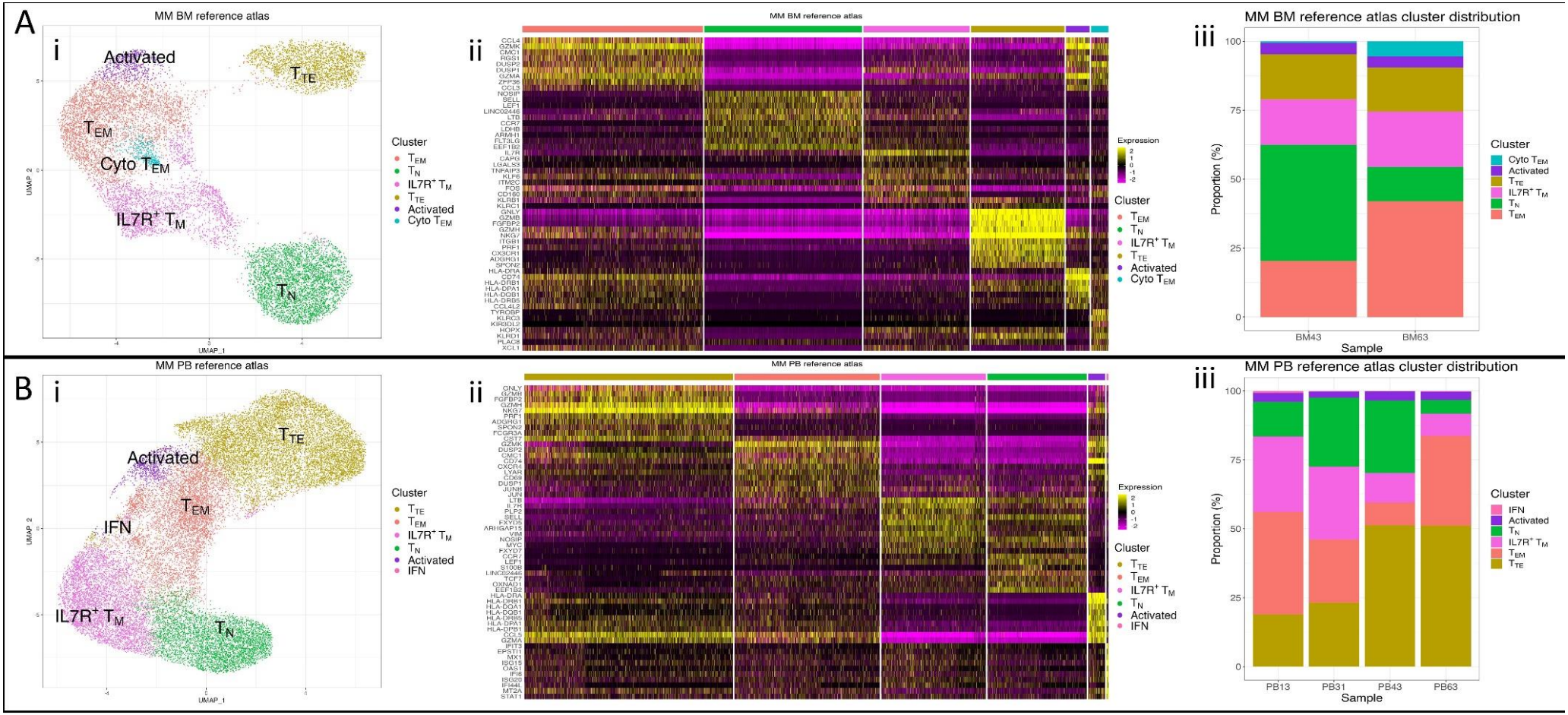

Supp. Figure 5: NDMM Reference atlases. (i) UMAPs, (ii) single-cell heat maps and (iii) bar plots of the MM reference atlases of the **A)** BM and **B)** PB. **i)** UMAPs demonstrate the identification of six clusters (annotated). **ii)** Heat maps illustrate transcriptional heterogeneity of CD8$^+$ T-cells. Each vertical line represents a single cell demonstrating the expression level, relative to the average expression level (upregulated = yellow, downregulated = purple) of the top 10 unique genes (y-axis) contributing to the transcriptional signature of each of the six identified clusters arranged by size of cluster (colored). **iii)** Bar plots show the number of cells (y-axis) contributing to each identified cluster (color) from each of the contributing samples.

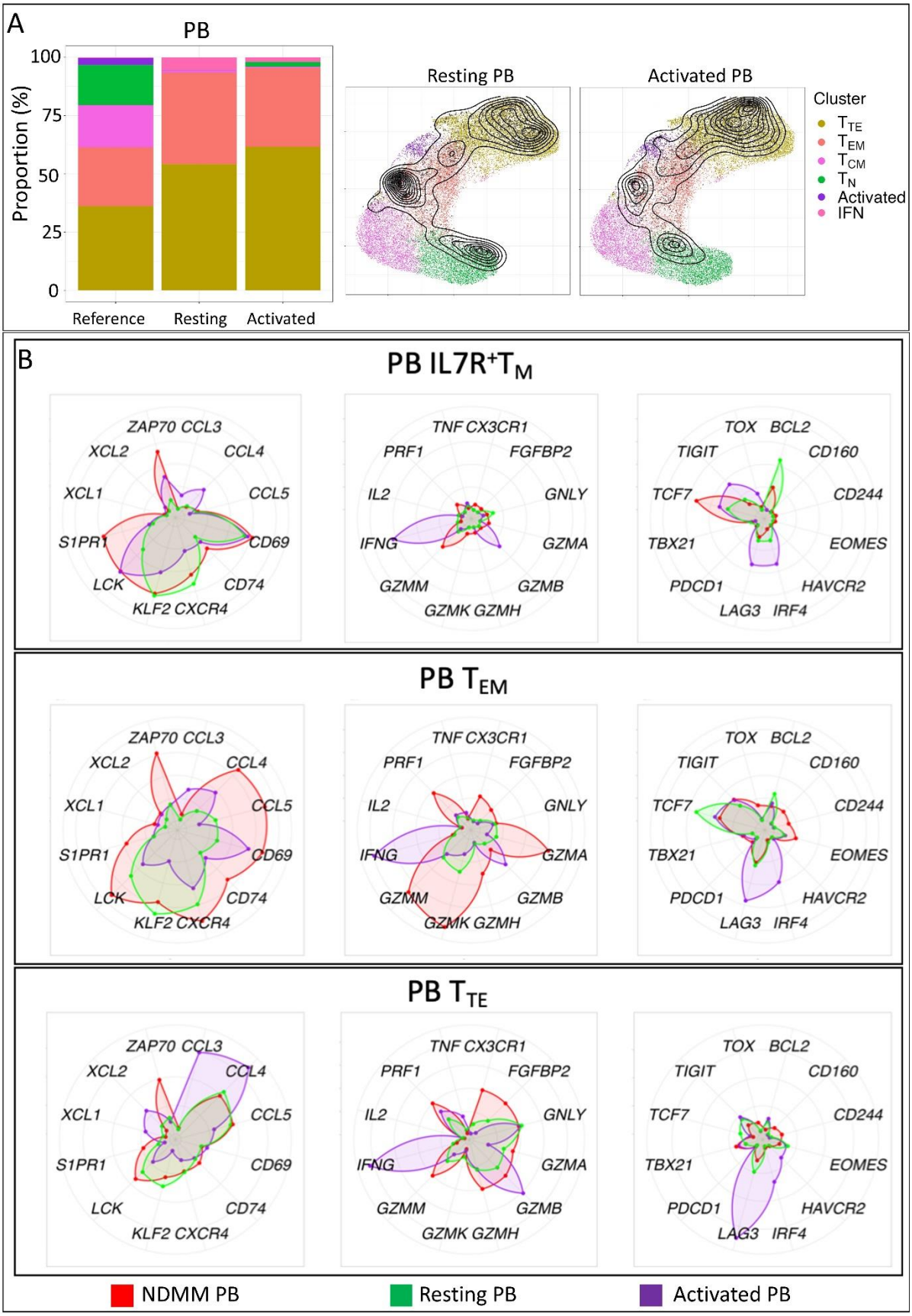

Supp. Figure 6. Results of ProjecTILs analysis of PB-CD8⁺ T-cells in multiple myeloma compared to age-matched healthy donors. A) ProjecTILs clustered CD8⁺ T-cells from the PB of NDMM patients (n = 4) into six clusters. Each dot represents a single cell colored according to cluster. Contour plots represent distribution of CD8⁺ T-cells from age-matched control data in resting (left) or TCR-activated states (right). The stacked bar graph illustrates cluster distribution of the reference atlas or controls data in resting (left) or TCR-activated states (right). **B) Radar plots** demonstrating expression levels of key genes related to TCR-activation and chemotaxis (left), effector function (middle) and T-cell exhaustion/ transcriptional regulators (right) of CD8⁺ T-cells from age-matched controls in TCR-activated (purple) or resting state (green) relative to the NDMM PB reference (red) across the IL7R⁺ T_M (top), T_{EM} (middle) and T_{TE} clusters (bottom).

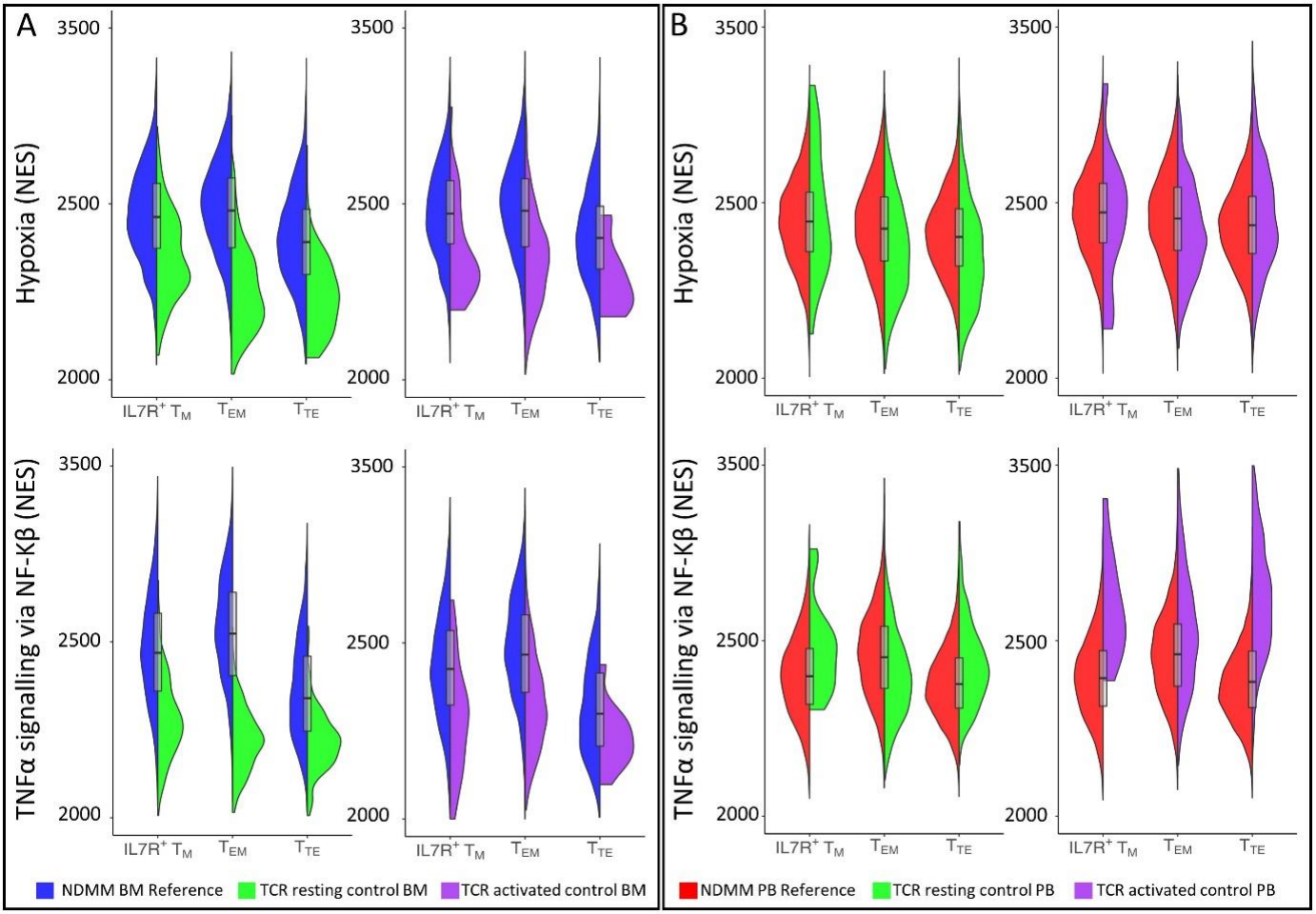

Supp. Figure 7: scGSEA results. A & B) Split violin plots showing enrichment toward the hallmark gene sets of hypoxia (top) and TNFα signaling via NF-κβ (bottom) in the BM reference (left, blue) and PB reference (right, red) compared to results from age-matched controls in resting (green) or TCR-activated (purple) states in the IL7R$^+$ T_M, T_{EM} and T_{TE} clusters. The median, upper and lower quartile are illustrated relative to cluster expression without segregation of sample.

Supplementary Tables

Supp. Table 1: List of mAbs used in flow cytometry

Marker	Clone	Conjugate	Supplier	Catalogue #
*CD45RA	HI100	BUV395	BD Biosciences	740298
CD8	RPA-T8	BUV496	BD Biosciences	564804
*CD69	FN50	BUV737	BD Biosciences	612817
CD4	SK3	BUV805	BD Biosciences	612887
*CD279 (PD-1)	EH12.1	BUV421	BD Biosciences	562516
*CD38	HIT2	BUV480	BD Biosciences	566137
*CD101	V7.1	BUV605	BD Biosciences	747548
*LAG-3	11C3C65	BUV650	Biolegend	369316
*TIGIT	741182	BUV711	BD Biosciences	747839
TCR Vαβ	T10B9.1A-31	BUV786	BD Biosciences	563825
*CD127	HIL-T7-M21	FITC	BD Biosciences	560549
*CD103	Ber-ACT8	BB700	BD Biosciences	745919
#CD25	2A3	PE	BD Biosciences	341009
CD197 (CCR7)	150503	PE-CF594	BD Biosciences	562381
CD57	HNK-1	PE-Cy7	Biolegend	359624
*KLRG1	SA231A2	APC	Biolegend	367716
!CD14	M5E2	AF700	BD Biosciences	557923
!CD19	HIB19	APCR700	BD Biosciences	564977
!CD56	NCAM16.2	APCR700	BD Biosciences	565139
*@#TCF-1	7F11A10	PE	Biolegend	655208
CD161	DX12	BV711	BD Biosciences	563865
CD183 (CXCR3)	1C6	BV421	BD Biosciences	562558
CD95 (FAS)	DX2	BB700	BD Biosciences	566542
@Granzyme B	GB11	FITC	BD Biosciences	560211
@Granzyme K	GM26E7	PE	BD Biosciences	370512
@Perforin	dG9	APC	Biolegend	308112
#IgG_1	X40	FITC	BD Biosciences	349041
#IgG_1	X40	PE	BD Biosciences	349043
#IgG_1	X40	APC	BD Biosciences	340442

**Used for FlowSOM clustering and tSNE visualisation; #Excluded from antibody cocktail; @Intracellular marker !Combined into DUMP channel to exclude cells not of interest.*
mAbs, monoclonal antibodies; BM, Bone Marrow; N/A, Not applicable; tSNE, t-distributed stochastic neighbour embedding.

Supp. Table 2: List of mAbs used in mass cytometry

Marker	Clone	Conjugate	Marker	Clone	Conjugate
CD160-AF647	BY55	N/A	CD122 (IL-2RB)	TU27	^{161}Dy
CD56	REA196	^{113}In	TCR V_β 21.3	IG125	^{162}Dy
CD8A	RPA-T8	^{115}In	CD183 (CXCR3)	REA232	^{163}Dy
CD57	HCD57	^{139}La	CD274 (PDL-1)	MIH1	^{164}Dy
CD49d*	9F10	^{141}Pr	TCR V_β 8$^{\#}$	56C5.2	^{165}Ho
CD19	HIB19	^{142}Ce	TIGIT	MBSA43	^{166}Er
CD45RA*	HI100	^{143}Nd	CD27	M-T271	^{167}Er
CD69*	FN50	^{144}Nd	Ki67$^{@}$	B56	^{168}Er
CD4	RPA-T4	^{145}Nd	CD25	M-A251	^{169}Tm
EOMES$^{@}$	WD1928	^{146}Nd	CD3	UCHT1	^{170}Yb
Cy5$^{\#}$	CY5-15	^{147}Sm	Granzyme B$^{@}$	GB11	^{171}Yb
CD28*	CD28.2	^{148}Sm	CD38*	HIT2	^{172}Yb
CD366 (Tim3)	7D3	^{149}Sm	Integrin B7	FIB504	^{173}Yb
KLRG1*	SA231A	^{150}Sm	TCR V_β 5.1	IMMU157	^{174}Yb
CD39*	A1	^{151}Eu	TCR V_β 13.1	IMMU222	^{174}Yb
CD45RO*	UCHL1	^{152}Sm	Perforin$^{@}$	B-D48	^{175}Lu
CD62L*	DREG-56	^{153}Eu	CD127*	A019D5	^{176}Lu
CD300a	P192	^{154}Gd	DNA1$^{@}$	N/A	^{191}Ir
CD137 (41BB)	4B4-1	^{155}Gd	DNA2$^{@}$	N/A	^{193}Ir
CD279 (PD-1)*	EH12.2H7	^{156}Gd	Cisplatin$^{@}$	N/A	^{194}Pt
CD300c	TX45	^{158}Gd	Cisplatin$^{@}$	N/A	^{195}Pt
CD197 (CCR7)	150503	^{159}Tb	Platinum	N/A	^{198}Pt
CD223 (Lag3)	17B4	^{160}Dy	T-bet$^{@}$	4B10	^{209}Bi

**Used for FlowSOM clustering and tSNE visualisation; @Intracellular marker; #used for AF647 detection. mAbs, monoclonal antibodies; N/A, Not applicable; tSNE, t-distributed stochastic neighbour embedding.*

mAbs, monoclonal antibodies; BM, Bone Marrow; N/A, Not applicable; tSNE, t-distributed stochastic neighbour embedding.

Supp. Table 3: Summary of recovered scRNA/TCR-Seq data following QC

Sample ID	Sample	Number of cell barcodes recovered	Ave. number of detected genes	Ave. number of recovered UMI	Mitochondrial genes (%)	Total TCR Clonotypes observed (n/%)	Cells with matching TCR data (n/%)
NDMM #013	[!]BM	7871	732	1625	1.90	4,455 (100)	6551 (83.2)
	PB	7822	1267	3966	4.10	3,876 (100)	7395 (94.5)
NDMM #031	[!]BM	2429	375	256	3.22	3,103 (100)	2317 (95.4)
	PB	7558	1098	3218	5.29	4,838 (100)	6559 (86.8)
NDMM #043	BM	7120	1005	3317	6.51	5,063 (100)	6869 (96.5)
	PB	6497	1097	3690	7.13	2,975 (100)	6207 (95.5)
NDMM #063	BM	7824	1251	3572	5.23	3,259 (100)	7472 (95.5)
	PB	6275	1374	3933	4.85	1,239 (100)	6147 (98.0)

[!]Gene expression library failed for this sample, excluded from analysis. QC, Quality Control; scRNA-Seq, single cell Ribonucleic acid sequencing; TCR, T-cell Receptor; ID, Identification; BM, Bone Marrow; PB, Peripheral Blood; UMI, Unique Molecular Identifier.

Excel files

Supp. Table 4: FindAllMarkers - DE results of the integrated analysis comparing one cluster against all other clusters

Supp. Table 5: GSEA results (Mann Whitney U test)

Supp. Table 6: FindMarkers - DE results of the integrated analysis comparing the same cluster across BM and PB

Supp. Table 7: GSEA results (Mann Whitney U test) - Age-matched vs. MM reference)

Supp. Table 8A - DE results MM vs. controls BM

Supp. Table 8B - DE results MM vs. controls PB

Please note, supplementary Tables 4, 6, and 8 are differential expression results from the R package "Seurat". The headers for these excel files are:

p_val : p-value (unadjusted).
avg_2logFC : log2 fold-change of the average expression between the two groups. Positive values indicate that the feature is more highly expressed in the first group.
pct.1 : The percentage of cells where the feature is detected in the first group.
pct.2 : The percentage of cells where the feature is detected in the second group.
p_val_adj : Adjusted p-value, based on bonferroni correction using all features in the dataset.

Supplementary tables 5 and 7 are Gene Set Enrichment Analysis results from the R package "escape". The headers for these excel files are:

rowname: The name of the gene set tested
T.statistic: t-statistic.
p.value: p-value (unadjusted).
FDR: False discovery rate
median.X: The normalised enrichment score for test X
median.Y: The normalised enrichment score for test Y

References

1. Zheng GX, Terry JM, Belgrader P, Ryvkin P, Bent ZW, Wilson R, Ziraldo SB, Wheeler TD, McDermott GP, Zhu J, Gregory MT, Shuga J, Montesclaros L, Underwood JG, Masquelier DA, Nishimura SY, Schnall-Levin M, Wyatt PW, Hindson CM, Bharadwaj R, Wong A, Ness KD, Beppu LW, Deeg HJ, McFarland C, Loeb KR, Valente WJ, Ericson NG, Stevens EA, Radich JP, Mikkelsen TS, Hindson BJ, Bielas JH. Massively parallel digital transcriptional profiling of single cells. Nat Commun. 2017 Jan 16;8:14049. Epub 2017/01/17. doi:10.1038/ncomms14049. Cited in: Pubmed; PMID 28091601.

2. Hao Y, Hao S, Andersen-Nissen E, Mauck WM, 3rd, Zheng S, Butler A, Lee MJ, Wilk AJ, Darby C, Zager M, Hoffman P, Stoeckius M, Papalexi E, Mimitou EP, Jain J, Srivastava A, Stuart T, Fleming LM, Yeung B, Rogers AJ, McElrath JM, Blish CA, Gottardo R, Smibert P, Satija R. Integrated analysis of multimodal single-cell data. Cell. 2021 Jun 24;184(13):3573-3587 e29. Epub 2021/06/02. doi:10.1016/j.cell.2021.04.048. Cited in: Pubmed; PMID 34062119.

3. McInnes LaH, John and Saul, Nathaniel and Grossberger, Lukas. UMAP: Uniform Manifold Approximation and Projection. The Journal of Open Source Software. 2018;3(29):861.

4. Andreatta M, Corria-Osorio J, Müller S, Cubas R, Coukos G, Carmona SJ. Interpretation of T cell states from single-cell transcriptomics data using reference atlases. Nature Communications. 2021 2021/05/20;12(1):2965. doi:10.1038/s41467-021-23324-4.

5. Szabo PA, Levitin HM, Miron M, Snyder ME, Senda T, Yuan J, Cheng YL, Bush EC, Dogra P, Thapa P, Farber DL, Sims PA. Single-cell transcriptomics of human T cells reveals tissue and activation signatures in health and disease. Nat Commun. 2019 Oct 17;10(1):4706. Epub 2019/10/19. doi:10.1038/s41467-019-12464-3. Cited in: Pubmed; PMID 31624246.

6. Aran D, Looney AP, Liu L, Wu E, Fong V, Hsu A, Chak S, Naikawadi RP, Wolters PJ, Abate AR, Butte AJ, Bhattacharya M. Reference-based analysis of lung single-cell sequencing reveals a transitional profibrotic macrophage. Nat Immunol. 2019 Feb;20(2):163-172. Epub 2019/01/16. doi:10.1038/s41590-018-0276-y. Cited in: Pubmed; PMID 30643263.

7. Borcherding N, Vishwakarma A, Voigt AP, Bellizzi A, Kaplan J, Nepple K, Salem AK, Jenkins RW, Zakharia Y, Zhang W. Mapping the immune environment in clear cell renal carcinoma by single-cell genomics. Commun Biol. 2021 Jan 27;4(1):122. Epub 2021/01/29. doi:10.1038/s42003-020-01625-6. Cited in: Pubmed; PMID 33504936.

8. Subramanian A, Tamayo P, Mootha VK, Mukherjee S, Ebert BL, Gillette MA, Paulovich A, Pomeroy SL, Golub TR, Lander ES, Mesirov JP. Gene set enrichment analysis: a knowledge-based approach for interpreting genome-wide expression profiles. Proc Natl Acad Sci U S A. 2005 Oct 25;102(43):15545-50. Epub 2005/10/04. doi:10.1073/pnas.0506580102. Cited in: Pubmed; PMID 16199517.

9. Vuckovic S, Bryant CE, Lau KHA, Yang S, Favaloro J, McGuire HM, Clark G, de St Groth BF, Marsh-Wakefield F, Nassif N, Abadir E, Vanguru V, McCulloch D, Brown C, Larsen S, Dunkley S, Khoo L, Gibson J, Boyle R, Joshua D, Ho PJ. Inverse relationship between oligoclonal expanded CD69- TTE and CD69+ TTE cells in bone marrow of multiple myeloma patients. Blood Adv. 2020 Oct 13;4(19):4593-4604. Epub 2020/09/29. doi:10.1182/bloodadvances.2020002237. Cited in: Pubmed; PMID 32986791.

10. Marsh-Wakefield F, Kruzins A, McGuire HM, Yang S, Bryant C, Fazekas de St Groth B, Nassif N, Byrne SN, Gibson J, Brown C, Larsen S, McCulloch D, Boyle R, Clark G, Joshua D, Ho PJ, Vuckovic S. Mass Cytometry Discovers Two Discrete Subsets of CD39(-)Treg Which Discriminate MGUS From Multiple Myeloma. Front Immunol. 2019;10:1596. Epub 2019/08/21. doi:10.3389/fimmu.2019.01596. Cited in: Pubmed; PMID 31428081.